Journal of Cultural Heritage 80 (2026) 246–252

Contents lists available at ScienceDirect

Journal of Cultural Heritage

journal homepage: www.elsevier.com/locate/culher

VSI: TECHNART 2025

Unveiling ancient maritime secrets through X-ray computed tomography (CT): Iron-based finds from the archaic shipwreck of Giglio-Campese

Cecilia Riccardizi[a,*], Matteo Bettuzzi[a], Maria Pia Morigi[a], Nayyab Amjad[a], Lucilla Fabrizi[b,c], Rosarosa Manca[b], Anna Mazzinghi[d], Alessandro Naso[e], Marco Benvenuti[b,f]

[a] *Department of Physics and Astronomy "Augusto Righi", University of Bologna, Bologna, Italy*
[b] *Department of Earth Sciences, University of Florence, Florence, Italy*
[c] *Museo "La Specola"-University Museums System, University of Florence, Florence, Italy*
[d] *Department of Physics and Astronomy, University of Florence, Sesto Fiorentino (Fi), Italy*
[e] *Department of Humanistic Studies, University of Naples Federico II, Naples, Italy*
[f] *Institute of Geosciences and Earth Resources, National Research Council, Pisa, Italy*

ARTICLE INFO

Article history:
Received 20 November 2025
Accepted 16 May 2026

Keywords:
X-ray computed tomography
X-ray fluorescence spectroscopy
Non-invasive analyses
Iron-based artifacts
Underwater archaeology
Archaic mediterranean trade

ABSTRACT

In August 1961 the remains of a shipwreck, dating back to the early 6th century BCE, were located at the Island of Giglio in the Bay of Campese (Tuscany, Italy), announcing a major archaeological discovery. Meticulous excavations carried out in the early 1980s partly brought to light both the exceptionally diverse cargo and structural remnants of the vessel. Owing to the extremely heterogeneous composition of the load of international scope, ranging from Etruscan to Greek productions, this finding reflects and testifies to the complexity of archaic trade networks across the Tyrrhenian Sea in the early 6th cent. BC. Within the framework of a broad multidisciplinary collaboration involving several institutions and experts, X-ray computed tomography (CT) was employed to investigate the hidden history of the ship and, by extension, aspects of our own cultural past. Among the numerous notable artifacts, the analysis concerned some heavily corroded and fragmented iron-based objects, whose original shape and function are no longer legible due to severe degradation and thick layers of concretions. To reconstruct their original morphology and thus identify the type of artifacts, two dedicated measurement campaigns were carried out in the *X-ray imaging* laboratory of the University of Bologna, Ravenna Campus (Emilia-Romagna, Italy), using a custom-designed CT system, equipped with a 200 kVp X-ray tube and a flat-panel detector with 127 µm pixel size. More than 20 tomographic scans were performed with a voxel size of about 100 µm, producing a substantial dataset for subsequent processing. The virtual removal of calcareous incrustations allowed us to formulate several hypotheses about the typology and function of the investigated artefacts. Preliminary interpretations have been proposed based on the observation of quadrangular cross-sectional profiles that originally contained metallic cores. These cores are now entirely or almost entirely consumed by corrosion, leaving only a layer of mineralized concretion with little to no metal preserved. Elemental composition was further assessed through complementary X-ray fluorescence (XRF) analyses, performed on selected points of the finds, supporting our investigation. Although the objects recovered from the depths of the Tyrrhenian Sea survive only as "ghosts" of their originals, the integration of CT imaging, visual inspection and XRF results has contributed to shed light on the ship's cargo composition of Greek and Etruscan provenance as well as on its route's stages.

* Corresponding author.
E-mail addresses: cecilia.riccardizi@unito.it (C. Riccardizi), matteo.bettuzzi@unibo.it (M. Bettuzzi), mariapia.morigi@unibo.it (M.P. Morigi), nayyab.amjad2@unibo.it (N. Amjad), lucilla.fabrizi@unifi.it (L. Fabrizi), rosarosa.manca@unifi.it (R. Manca), anna.mazzinghi@unifi.it (A. Mazzinghi), alessandro.naso@unina.it (A. Naso), m.benvenuti@unifi.it (M. Benvenuti).

https://doi.org/10.1016/j.culher.2026.05.017
1296-2074/

1. Introduction and research aim

The shipwreck of Giglio-Campese, discovered at a depth of 50 meters off Giglio Island (Tuscany, Italy), dates to the early 6th century BCE (580–570 BCE) and represents a pivotal source for reconstructing Archaic Mediterranean trade routes. In the 1980s, Mensun Bound, later a leading underwater archaeologist, directed a meticulous excavation uncovering the ship's structural remains and its remarkably diverse and international cargo [1]. The relevance of the shipwreck emerged immediately, as it was one of the earliest known in the Mediterranean [1]. The origin of the ship remains still debated, as both an Etruscan and Greek affiliation might be invoked considering the site of discovery and the cargo composition. Although the excavation remained incomplete, as for most archaic shipwrecks currently known in the Mediterranean [2], this discovery has yielded an extraordinary body of evidence, significantly contributing to the study of Archaic trade networks across the Tyrrhenian Sea [1,3]. The numerous sensational samples open new perspectives not only on trade and material culture but also on technological innovation and craft production of the time, as testified by the discovery of a wooden vernier caliper, previously unknown before the Medieval period [3].

Considering the significance of the recovery, in 2019 a project aimed at studying the exceptional findings was launched, establishing a broad multidisciplinary collaboration coordinated by the University of Naples Federico II [4].

Among the artifacts, some highly corroded iron-based conglomerates were also part of the precious cargo. Degradation phenomena and thick layers of marine concretions affect these objects, whose peculiar shape hinders the original features. X-ray computed tomography (CT) has, therefore, been proposed, in combination with X-ray fluorescence (XRF) investigation, as well-established method to get insights into the hidden past of the corroded findings in a completely non-invasive way [5–8]. Indeed, CT analyses produce high-resolution two-dimensional images representing sections of the object at different depths, from which the 3D volume of its inner structure can be easily obtained [9]. Thus, it is possible to virtually remove the layer of corrosion and examine the concealed morphology that would otherwise remain inaccessible. On the other hand, XRF provides valuable data on the elemental composition of the samples [10]; only qualitative information was significant in this case due to the high level of corrosion of the metal which hinders the chemical characterization of the original alloy. By integrating the imaging results with the compositional information, our study seeks to reconstruct the original morphology of some seemingly shapeless iron fragments recovered from the depths of the Tyrrhenian Sea, revealing no longer recognizable features and suggesting possible functions. Beyond individual artifacts, this research aims at contextualizing the findings within broader maritime trade and craft production in the early 6th-century BCE Mediterranean world.

2. Material and methods

2.1. Studied materials

The analysed samples were selected from a variety of iron-based conglomerates, considering their size, shape, and radiopacity. Each sample features layers of marine concretion of varying thickness, within which, in some cases, objects of different nature, such as stones, wood and clay materials, have been incorporated. Some fragments, although found separately, seem to belong to a more complex structure. Multiple scans were necessary for this object (Sample 1), which is made up of nine components that were scanned separately. Overall, 13 distinct objects were investigated, from which 3 representative artifacts (Fig. 1) were selected for presentation in this paper. These are hereafter referred to as Sample 1, 2, and 3, respectively. Their selection was based on morphological complexity and the presence of informative structural features, such as the shape of the inner sections. The remaining objects were either too radiopaque or showed fewer interesting characteristics (a complete overview is provided in the Supplementary Material).

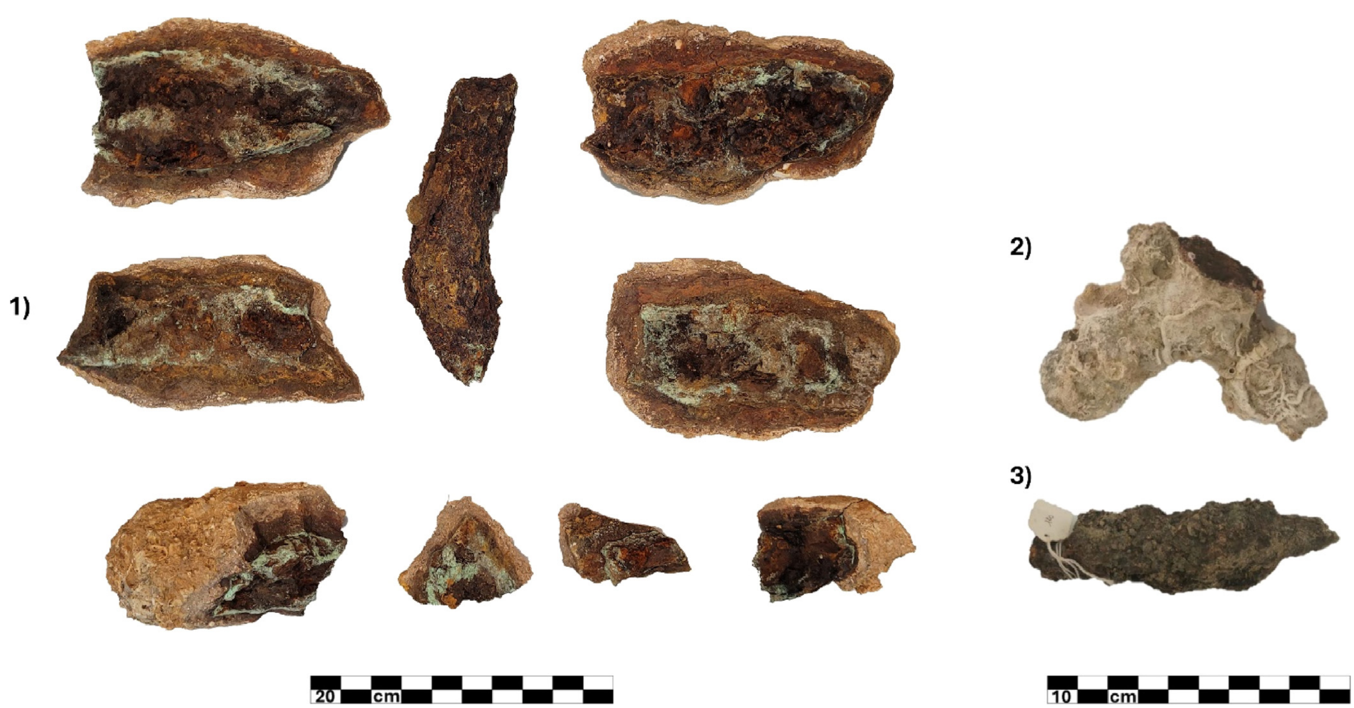

Fig. 1. The three representative iron-based artifacts from the Archaic Shipwreck of Giglio-Campese selected for this paper. Sample 1 consists of 9 separately recovered fragments of a single object, shown from the inner sides, where the presence of green patinas can also be appreciated.

Table 1
Scanning parameters used in this study.

	Sample 1	Sample 2,3
Tube voltage	200 kV	160 kV
Tube current	3.5 mA	4 mA
Beam filtration	2 mm Cu	1 mm Fe
Detector frame rate	5 fps	5 fps
Frame average	8	4
Number of projections	900	900
Angular range	360 deg	360 deg
Detector pixel size	0.127 mm	0.127 mm
Source-detector distance	1617 mm	1840 mm
Source-object distance	1470 mm	1480 mm
Object-detector distance	147 mm	360 mm
Magnification	1.10	1.24
Voxel size	0.1155 mm	0.1021 mm

2.2. CT system and data acquisition

The samples were analysed during two dedicated measurement campaigns, both carried out in the *X-ray imaging* laboratory of the University of Bologna, Ravenna Campus, using a custom-designed CT system, which is suitable for both on-site and laboratory investigations. This system is typically used for scanning large or highly attenuating objects, as in the present study. The experimental setup consists of a COMET Yxlon EVO 200D X-ray tube (maximum voltage: 200 kV, maximum current: 6 mA, focal spot size: 1 mm) and a Varian PaxScan 2520D indirect-conversion flat panel detector (CsI:TI scintillator). The detector features a sensitive area of 19.5×24.4 cm^2 (1536×1920 pixels) and high spatial resolution (127 µm pixel size), providing a maximum achievable voxel size of about 100 µm. The detector is placed on an X-Y translation stage that allows the field of view to be extended up to 150×150 cm^2, while the source is mounted on a 130 cm vertical translation axis. A Physik Instrumente Micos PRS200 rotary platform is positioned between the X-ray tube and the detector, supported by a three-foot iron stage. The platform enables 360° rotation of the samples and can support weights up to 50 kg [11].

Due to the high X-ray attenuation of the investigated materials, the tube was operated at its maximum voltage in some cases. The use of metallic filters further improved the signal by blocking low-energy X-rays. Table 1 lists the complete set of acquisition parameters. Under these conditions, beam hardening effects were substantially reduced; therefore, no Beam Hardening Correction (BHC) was applied. For Samples 2 and 3, a frame averaging value of 4, instead of 8, was chosen mainly in view of the large number of scans required during the second measurement campaign. This setting provided a suitable compromise between signal-to-noise ratio (SNR), which was already high for the detector used (see Supplementary Material for the SNR curve), and total acquisition time, while preserving reconstruction quality.

Overall, over 20 tomographic scans were performed at a voxel size of approximately 100 µm, producing a substantial dataset for further processing.

Image reconstruction was performed using PARREC (PARallel REConstruction), a dedicated software developed by Professor Rosa Brancaccio at the Department of Physics and Astronomy “Augusto Righi” of the University of Bologna, based on the cone-beam algorithm of Feldkamp, Davis, and Kress (FDK) [12].

Three-dimensional renderings were produced with VGStudio MAX 2.1 (by Volume Graphics) and further elaboration of the CT images was done using the open-source software Fiji (ImageJ).

2.3. XRF system and data acquisition

For XRF analysis, the INFN-CHNet instrument, thoroughly described by Taccetti et al. in [10], was employed for this study. It is a highly transportable device specifically designed for cultural heritage applications. In short, the measuring head has an X-ray tube (Moxtek, 40 kV maximum voltage, 0.1 mA maximum anode current), a silicon drift detector (Amptek XR100 SDD), and a telemeter (Keyence IA-100) for the adjustment of the sample–instrument distance. The head is installed on three linear motor stages by Physik Instrumente. An in-house developed software controls the instrument operation and data analysis. The operating conditions of the X-ray tube were 40 kV anode voltage, 40 µA filament current, Mo anode with an 800 µm diameter collimator. Measurements lasted 120 s.

3. Results

3.1. CT results

The most representative outcomes of the two tomographic campaigns are presented below.

All reported distances, measured on CT slices, are affected by an uncertainty comparable to the voxel size ($\approx$ 0.1 mm). Fig. 2 illustrates the main results of the tomographic reconstruction and 3D rendering process of 9 fragments, which, based on visual inspection, appeared to belong to the same artifact (Sample 1). Each fragment was reconstructed individually; subsequently, the 3D modelling enabled the virtual reassembly of the object as well as the digital removal of calcareous incrustations (Fig. 2a–b). The rendering tools, such as the possibility of making virtual cuts in any direction, allowed us to reveal the presence of a well-defined quadrangular section (with maximum dimension of 2.5×3.0 cm^2), tapering toward the end (Fig. 2c). Furthermore, a more radio-opaque outline became clearly visible. This outline corresponds to the areas which appear green to the naked eye (Fig. 1) and from which XRF analysis revealed the presence of high amounts of Cu (Fig. 4, Section 3.2): this led us to hypothesize that Sample 1 is a bimetallic object, consisting of an iron core covered with a thin (<1 mm) copper-based layer. One of the fragments (at the centre of Sample 1 in Fig. 1) stands out for its particularly high radiopacity, reflecting its strong X-ray absorption. This element may have originally occupied the central position of the object, although it could not be fitted back into the reconstructed volume (Fig. 2c), most likely due to morphological alterations and volumetric changes it has undergone over time. Unlike the other pieces, it is free from calcareous encrustations, suggesting the possibility that the fragmentation of the object occurred during the post-excavation phase.

Fig. 3 illustrates the CT scan of 2 apparently similar finds (Samples 2 and 3, see Fig. 1) whose original shape is entirely obscured by the external concretion. The tomographic slices, however, provided crucial insights. Sample 2 consists of two elements bound together by concretions, as revealed in coronal views at different depths, both with well-defined square sections, while Sample 3 appears as an elongated object with a circular cross-section of variable diameter. Both preserve the geometrical outline of their cores despite extensive mineralization. They also reveal complex inner structures, likely related to an advanced corrosion of the original metal core, now transformed into a highly degraded, wood-like, fibrous material (Fig. 3).

CT imaging revealed that the corrosion thickness varies significantly among the fragments, with values on the order of a few millimetres, ranging approximately from 3.0 to 11.0 mm. The corresponding relative uncertainty is estimated to be approximately 1–3%, consistent with the voxel size. Accurate quantification, however, is limited by the partial overlap between corrosion layers and residual metallic structures.

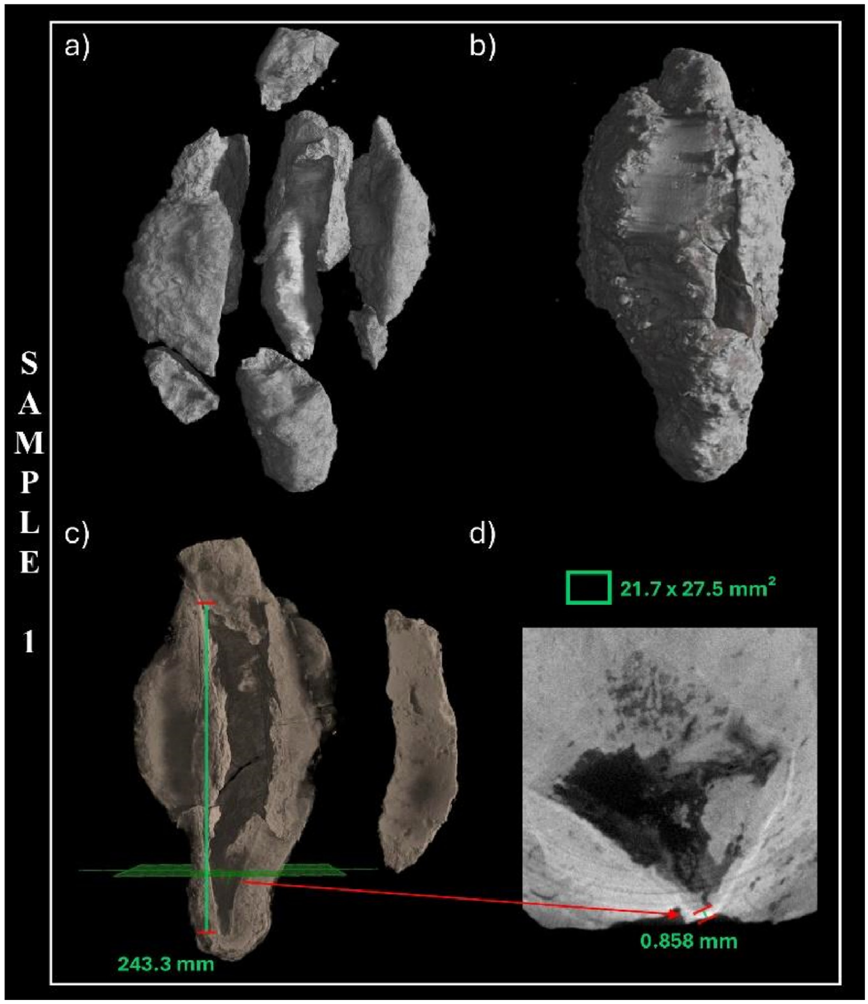

Fig. 2. Tomographic reconstruction and 3D rendering for Sample 1. a) 3D model of the individual fragments during the virtual reassembling of the complete volume, shown in b). c) Vertical cut, after the virtual removal of marine concretions; note that the element on the right could not be inserted into the reconstructed volume, where it probably was originally. d) Axial slice showing a well-defined quadrangular section with a ∼1mm-thick, more radiopaque contour.

3.2. XRF results

XRF analysis was performed on the calcareous incrustations, the corrosion areas, and the metallic profiles, when accessible. Complete results are reported in Table S4 in the Supplementary Material. Iron was confirmed as the main element in the exposed metallic and corroded areas (Fig. 4). S, Cl, Ca and low amounts of Mn, and Cu were also identified in variable amounts in most areas and should be related to the corrosion process. Trace amounts of Si, K, Zn and As/Pb, were also detected in a few spots.

As mentioned above, the spectra obtained from the green layer of Sample 1 were characterised by a strong increase in the Cu signal (Fig. 4), indicating a Cu-based material rather than iron corrosion products like green rust [13]. Neither Sn, Zn, nor Pb, typical components of Cu alloys, were detected (Fig. 4).

Calcium, often associated with Sr, was the main element in the concretions; low amounts of Si, P, S, K, Fe, and Cu were also detected (Fig. 4).

4. Discussion

The virtual removal of the encrustation layers proved crucial for reconstructing the original morphology of the artifacts and for attempting a typological identification. In most cases, the tomographic analysis suggests that the profiles were originally occupied by metal cores which are now almost entirely lost: in a few samples, the core is void, while in others it survives only as a fibrous residue, likely the product of advanced corrosion processes [14–18]. The virtual reassembly of the nine fragments attributed to Sample 1 allowed us to confirm that they belonged to the same object. Particularly noteworthy, is the identification, through CT and XRF analyses, of a thin external copper layer covering the entire object. This finding suggests that Sample 1 was deliberately manufactured as a bimetallic artifact [13], as contamination from the marine environment or from adjacent Cu-bearing objects would be unlikely to produce such a uniform distribution on all sides of the object.

Copper plating on iron was practiced since the earliest use of iron, even if it is not so commonly documented, particularly in contexts as early as the Giglio-Campese shipwreck; it had an aesthetic and protective function, since the copper plating created a barrier against corrosion [19]. Through the time it could be applied on a variety of objects, such as bridle bits, iron bells, padlocks, stirrups, sword hilts, spearheads, bowls, tripods, and, more in general, to objects exposed to weathering and/or with a distinct ceremonial or aesthetic value [19–21]. Regarding Sample 1, which has emerged as the most significant find in our set, the reconstructed shape (Fig. 2) is not easily attributable to a specific ar-

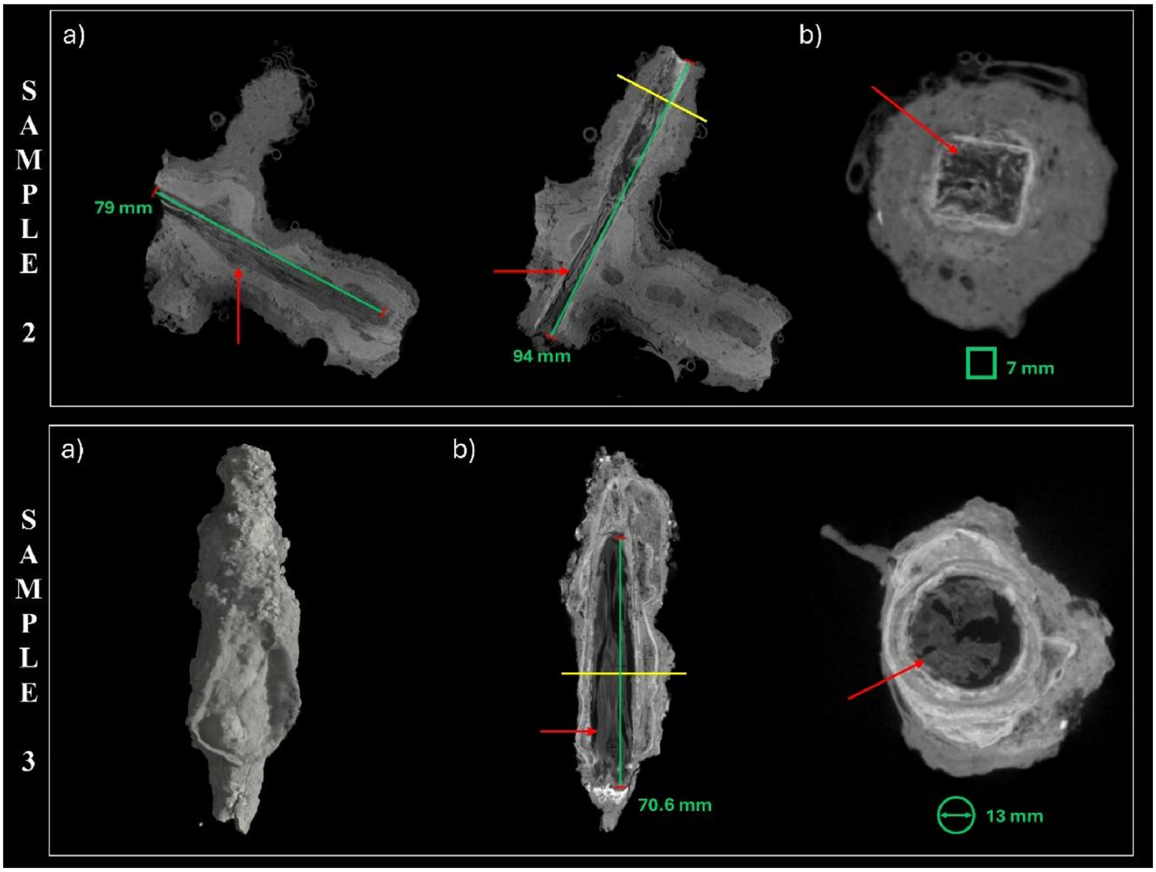

Fig. 3. Tomographic reconstruction and 3D rendering for Samples 2 and 3. Sample 2: a) Coronal slices at different depths showing 2 elements held together by concretions. b) Axial slice showing a 7 mm square section. Sample 3: a) 3D model of the elongated object. b) Slices showing a profile with a circular section. Yellow lines indicate the plane corresponding to the displayed axial slices. Red arrows mark the internal corrosion structures.

tifact. Its peculiar shape and its discovery on a shipwreck allow for a tentative association of this object with navigation, possibly as a tool of considerable value in maritime contexts, which would have necessitated protection from environmental degradation. A definitive interpretation, however, would necessitate a direct comparison with a better-preserved example.

Objects with analogous characteristics are notably rare, particularly within the specific chronological framework under analysis. Leading instances of synthetic surface layers are found on Bronze Age daggers and vessels recovered from Mycenaean shaft graves and various sites across Greece. Furthermore, a substantial body of Egyptian and Roman artefacts featuring metallic inlays has been recognised as deliberately patinated over recent decades [22]. Considering the chronological context of our shipwreck, the practice of surface treatment was certainly established; however, it was predominantly observed for artefacts of aesthetic or ceremonial significance. Drawing direct comparisons remains challenging: such objects were either clad in bronze—a material well-renowned for its ritual and decorative utility, as seen in the iron bowls (dated from 9th to early 7th centuries BC) analysed by Ashkenazi et al. (2012)—or featured very limited laminated surfaces intended for decoration, such as the axe studied by Berger (2015).

Regarding finds entirely encased in other metals, as seen in Sample 1, the historical use of gold foil on various materials is more documented, primarily to enhance economic and aesthetic value in ritual and decorative artefacts [23]. However, given that our object is instead entirely covered in a layer likely composed essentially of copper—with no significant traces of tin (Sn) or arsenic (As) typically found in other bronze surface coatings—its primary purpose appears to have been functional rather than aesthetic. Such cladding would have provided vital corrosion protection for an iron structural maritime component constantly exposed to water.

The closest parallels are found in land-based Iron Age contexts, specifically iron bridle bits plated in copper. However, these have been recovered mainly from Northern European sites, such as those in the UK [19,24] or the renowned site of La Tène in Switzerland, the latter dating to the phase between 450 and 390 BCE [25].

To the best of our knowledge, the most similar object found in Italy is considerably more recent. Discovered at the medieval site of Peveragno (Piedmont, North-western Italy) and dated to the 5th or 6th century AD, this find also remains typologically unidentified. Invasive analyses involving sampling identified it as consisting of a near-homogeneous copper layer presenting a thickness below 1 mm and covering an iron core [26]. In that instance, too, the object was interpreted as a utilitarian tool where the plating served as a barrier against corrosion rather than for decorative purposes.

The presence of a radiopaque outer contour was also observed in most of the other samples, suggesting that metallic components may have migrated during degradation, further complicating the distinction between the original structure and secondary concretion. However, only Sample 1 showed a distinct composition between the metallic profile and the thick corroded areas.

Whilst further investigations will undoubtedly be required to fully ascertain the nature of Sample 1, it appears to be a functional object that predates any currently known parallels, at least within an Italian context. Future comparisons with similar artefacts will certainly help to clarify where and how these objects were man-

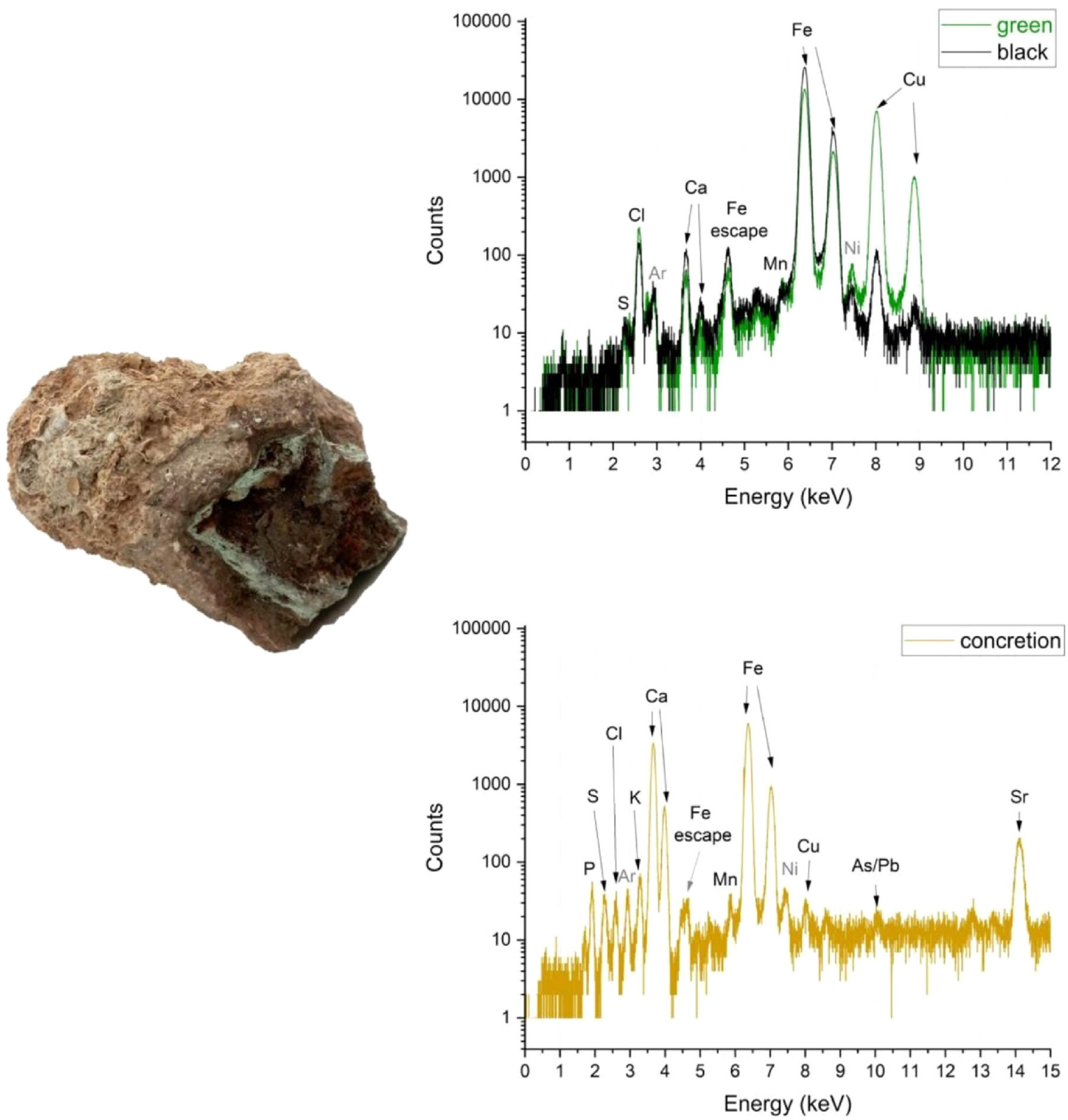

Fig. 4. Representative XRF spectra from the black core, the green layer and the calcareous concretion of one of the fragments composing Sample 1. Ar and Ni are labelled in grey as they are related to contamination from air and the equipment, respectively.

ufactured and for what specific purposes, thereby shedding light on ancient practices and Mediterranean trade routes. At present, however, the scarcity of such finds precludes further hypotheses.

In this panorama, determining the nature of the coatings of Sample 1 is essential, not only for the preservation of the extant material but also for its aesthetic restoration and archaeological contextualisation. This could represent one of the earliest instances of copper-plated iron objects, at least within the Italian archaeological record.

Beyond Sample 1, morphological observations on the other analysed objects also provided useful archaeological indications. Several finds, such as Sample 2, exhibit small square cross-sections, only a few millimetres across, consistent with those of iron spits [27]. It is interesting to note that according to the archaic Greek literature, metal spits not only served cooking purposes but might also carry a pre-monetary value [28], thereby connecting these artifacts to economic practices.

Other fragments, by contrast, display circular or pointed sections, like those observed in Sample 3, which suggests that they may instead represent weapon components, such as arrowheads or blades.

5. Conclusions

The proposed case study highlights the significance of scientific methods and interdisciplinary collaboration in attaining a comprehensive and precise understanding of underwater cultural heritage and, ultimately, our past. The use of non-invasive techniques is particularly relevant in underwater archaeology and conservation, where direct sampling or mechanical cleaning of artefacts is often not feasible without risking irreversible damage. Although CT is a well-established method for the investigation of terrestrial archaeological materials [29–30], its application to marine artefacts remains less widespread. This is partly due to the presence of thick concretions and heterogeneous corrosion products, which can complicate image acquisition and interpretation. Nevertheless, previous studies on shipwreck artefacts [31] have demonstrated the strong potential of CT in this field. In this context, the integration of computed tomography with chemical analysis has been instrumental in investigating heavily degraded marine artifacts from the 6th-century BCE Giglio Campese shipwreck. The tomographic reconstruction revealed that most of the iron-based samples survive only as residual traces of the original objects, preserved through a complex mixture of corrosion products and calcareous deposits from the marine environment. XRF complemented these findings, confirming the material compositions. This approach enabled the identification of possible morphologies and functional types, such as spits or weapons, for most of the investigated samples. Further studies could focus on the detailed characterization of the corrosion products in order to inform future conservation treatments. Moreover, the integration of complementary techniques, such as synchrotron-based X-ray methods and neutron imaging, would be particularly valuable for the study of highly radiopaque conglomerates, especially when organic materials are also embedded [6,11]. Future investigations of additional artefacts from the shipwreck would also contribute to a more comprehensive archaeological interpretation of the cargo and its preservation state. Beyond the individual objects, the study demonstrates the broader value of multidisciplinary archaeometric approaches for refining our understanding of archaic trade networks and material culture carried across the Mediterranean Sea.

Funding sources

This work has been partially financially supported by the project PE5 CHANGES: Cultural Heritage Active Innovation for Sustainable Society. PE 0000020 CHANGES, CUP [J33C22002850006], PNRR Missione 4 Componente 2 Investimento 1.3, NextGenerationEU.

Acknowledgements

We thank the Soprintendenza Archeologia, Belle Arti e Paesaggio per le Province di Siena, Grosseto e Arezzo for granting authorization for the analyses.

Supplementary materials

Supplementary material associated with this article can be found, in the online version, at doi:10.1016/j.culher.2026.05.017.

References

[1] M. Bound, The Giglio Wreck, A Wreck of the Archaic Period (c.600 BC) Off the Tuscan island of Giglio. An account of Its Discovery and Excavations: A Review of the Main Finds, Hellenic Institute of Marine Archaeology, 1991 Volume ENAΛIA Supplement 1.
[2] P. Pomey, Ships and shipping, in: A. Naso (Ed.), Etruscology, De Gruyter, Berlin, Boston, 2017, pp. 371–389.
[3] E.M. Giuffré, M. Milletti, A. Naso, J. Tabolli, A. Zifferero, Il relitto arcaico del Giglio-Campese, Ann. Fond. Faina Mus. «Claudio Faina» 29 (2025) 265–284.
[4] E. Rizzo, M. Morelli, C. Melchiorre, A. Naso, A. Amoresano, A. Carpentieri, The scent of an archaic wreck: minimally invasive characterisation of archaeological finds, Rend. Lincei. Sci. Fis. Nat. 35 (2024) 719–724, doi:10.1007/s12210-024-01260-x.
[5] M. Albahri, A. Barifcani, D. Dwivedi, S. Iglauer, M. Lebedev, I. Macleod, L. Machuca, X-ray micro-computed tomography analysis of accumulated corrosion products in deep-water shipwrecks, Mater. Corros. 70 (2019) 1977–1998, doi:10.1002/maco.201910842.
[6] H.J. Simon, G. Cibin, C. Reinhard, Y. Liu, E. Schofield, I.C. Freestone, Influence of microstructure on the corrosion of archaeological iron observed using 3D synchrotron micro-tomography, Corros. Sci. 159 (2019) 108132, doi:10.1016/j.corsci.2019.108132.
[7] M. Ferretti, The investigation of ancient metal artefacts by portable X-ray fluorescence devices, J. Anal. At. Spectrom. 29 (2014) 1753–1766, doi:10.1039/C4JA00107A.
[8] G. Degenhart, S. Wagner, P. Tropper, U. Töchterle, M. Auer, The 3D visibility of rust: micro computed tomography investigations of a roman iron nail from Aguntum, Minerals (2025) 15, doi:10.3390/min15090939.
[9] F. Albertin, M. Bettuzzi, R. Brancaccio, M.P. Morigi, F. Casali, X-ray computed tomography In situ: an opportunity for museums and restoration laboratories, Heritage 2 (2019) 2028–2038, doi:10.3390/heritage2030122.
[10] F. Taccetti, L. Castelli, C. Czelusniak, N. Gelli, A. Mazzinghi, L. Palla, C. Ruberto, C. Censori, A. Lo Giudice, A. Re, et al., A multipurpose X-ray fluorescence scanner developed for in situ analysis, Rend. Lincei. Sci. Fis. Nat. (2019) 30, doi:10.1007/s12210-018-0756-x.
[11] A. Mazzinghi, L. Castelli, C. Ruberto, S. Barone, F. García-Avello Bofías, A. Bombini, C. Czelusniak, N. Gelli, F. Giambi, M. Manetti, et al., X-ray and neutron imaging for cultural heritage: the INFN-CHNet experience, Eur. Phys. J. Plus 139 (2024) 635, doi:10.1140/epjp/s13360-024-05429-z.
[12] R. Brancaccio, M. Bettuzzi, F. Casali, M.P. Morigi, G. Levi, A. Gallo, G. Marchetti, D. Schneberk, Real-time reconstruction for 3-D CT applied to large objects of cultural heritage, IEEE Trans. Nucl. Sci. 58 (2011) 1864–1871, doi:10.1109/TNS.2011.2158850.
[13] D.A. Scott, G. Eggert, Iron and Steel in Art: Corrosion, Colorants, Conservation, Archetype, 2009.
[14] E. Estalayo, J. Aramendia, J.M. Matés Luque, J. Madariaga, Chemical study of degradation processes in ancient metallic materials rescued from underwater medium, J. Raman Spectrosc. 50 (2019) 289–298, doi:10.1002/jrs.5553.
[15] M. Bernabale, F. Cognigni, L. Nigro, M. Rossi, T. de Caro, C. De Vito, A comprehensive strategy for exploring corrosion in iron-based artefacts through advanced Multiscale X-ray microscopy, Sci. Rep. 12 (2022) 6125, doi:10.1038/s41598-022-10151-w.
[16] D. Ashkenazi, E. Mentovich, D. Cvikel, O. Barkai, A. Aronson, Y. Kahanov, Archaeometallurgical investigation of iron artifacts from shipwrecks – a review, in: Archaeology, New Approaches in Theory and Techniques, Intech, Ollich-Castanyer, I., Ed, 2012, pp. 169–186.
[17] J. Moore, Long-term corrosion processes of iron and steel shipwrecks in the marine environment: a review of current knowledge, J. Marit. Archaeol. 10 (2015), doi:10.1007/s11457-015-9148-x.
[18] A.L. Grevey, V. Vignal, H. Krawiec, P. Ozga, K. Peche-Quilichini, A. Rivalan, F. Mazière, Microstructure and long-term corrosion of archaeological iron alloy artefacts, Herit. Sci. 8 (2020) 57, doi:10.1186/s40494-020-00398-9.
[19] M. Corfield, Copper plating on iron, in: S. La Niece, P. Craddock (Eds.), Metal Plating and Patination, Butterworth-Heinemann, 1993, pp. 276–283.
[20] E. Asderaki-Tzoumerkioti, T. Rehren, Z. Malakasioti, Bronze-plated iron bowls from early Iron age Central Greece, in: ISA 2006: 36th International Symposium on Archaeometry 2006, 2009, pp. 383–390.
[21] L. Cappuccini, M. Milletti, Rex Rusellarum, Le Tombe Principesche Di Sassi Grossi e La Nascita Di Roselle, All'insegna del Giglio s.a.s, Sesto Fiorentino (FI), 2024.
[22] D. Berger, Artificial patination in early Iron Age Europe: an analytical case study of a unique bronze artefact, J. Archaeol. Sci. 57 (2015) 130–141, doi:10.1016/j.jas.2015.01.025.
[23] A. Giumlia-Mair, Plating and surface treatments on ancient metalwork, Adv. Archaeomaterials 1 (2020) 1–26, doi:10.1016/j.aia.2020.10.001.
[24] J. Watson, G. Edwards, Conservation of Material from Anglo-Saxon Cemeteries in Anglo-Saxon Cemeteries, A Reappraisal, E. Southworth (Ed.), Alan Sutton: Stroud, 1990.
[25] P. Vouga, La Tène; Monographie De La Station Publiée Au Nom De La Commission Des Fouilles De La Tène, Hiersemann: Leipzig, 1923.
[26] G.M. Ingo, E. Angelini, E. Micheletto, G. Chiozzini, G. Bultrini, T. De Caro, Copper plating on an iron artefact from the early medieval site of Peveragno (Piemonte, north western Italy), BAR Int. Ser 1043 (2002) 383–387.
[27] C. Kohler, Die obeloi der Heuneburg, in: W. Kimmig (Ed.), Importe Und Mediterrane Einflüsse auf Der Heuneburg, von Zabern: Mainz, 2000, pp. 197–213.
[28] N. Parise, in: La Nascita Della moneta. Segni premonetari e Forme Arcaiche Dello Scambio, Roma, Donzelli, 2000, pp. 32–39.
[29] A. Re, J. Corsi, M. Demmelbauer, M. Martini, G. Mila, C. Ricci, X-ray tomography of a soil block: a useful tool for the restoration of archaeological finds, Herit. Sci. 3 (2015), doi:10.1186/s40494-015-0033-6.
[30] A.C. Fariselli, S. Fiorentino, M.P. Morigi, M. Bettuzzi, I. Rimondi, K. Doppiu, M. Vandini, Archaeometric analyses and restoration of silver jewellery from the Punic Necropolis of Tharros – Capo San Marco (Sardinia, Italy), Int. J. Conserv. Sci. 13 (2022) 771–792.
[31] A. Pakzad, F. Iacoviello, A. Ramsey, R. Speller, J. Griffiths, T. Freeth, A. Gibson, Improved X-ray computed tomography reconstruction of the largest fragment of the Antikythera Mechanism, an ancient Greek astronomical calculator, PLoS One (2018) 13, doi:10.1371/journal.pone.0207430.